CHEMISTRY
A EUROPEAN JOURNAL

DOI: 10.1002/chem.200700131

Giant Porphyrin Disks: Control of Their Self-Assembly at Liquid–Solid Interfaces through Metal–Ligand Interactions

Marga C. Lensen,[a, b] Johannes A. A. W. Elemans,*[a] Sandra J. T. van Dingenen,[a] Jan W. Gerritsen,[a] Sylvia Speller,[a] Alan E. Rowan,*[a] and Roeland J. M. Nolte[a]

Abstract: The synthesis and self-assembly behaviour of porphyrin dodecamers $\mathbf{1}H_2$ and Zn–**1**, which consist of twelve porphyrins that are covalently attached to a central aromatic core, is described. According to STM, 1D and 2D NMR studies, and molecular modelling calculations, the porphyrin dodecamers have a yo-yo-shaped structure. Their large π surface, in combination with their disk-like shape, allows them to form self-assembled structures, which in the case of Zn–**1** can be tuned by adding bidentate ligands. The self-assembly of the molecules at the liquid–solid interface of 1-phenyloctane with highly oriented pyrolytic graphite or Au(111) was imaged by using STM. The porphyrin disks in the self-assembled arrays have an edge-on orientation on the surface. The addition of bidentate axial ligands to the Zn–**1** molecules in the arrays allows their intermolecular distance to be precisely controlled.

Keywords: metal–ligand coordination · porphyrinoids · scanning tunneling microscopy · self-assembly · surface chemistry

Introduction

In recent years the design and construction of multi-chromophoric arrays has become very popular in the field of supramolecular chemistry with many potential applications in materials science.[1] Arranging chromophores in an ordered fashion enables the construction of new materials that can exhibit unique photophysical and (opto)electronic properties as a result of excitonic interactions between adjacent dye units.[2] By using the structure of a natural light-harvesting system as a blueprint,[3] many studies have been dedicated to constructing artificial highly ordered porphyrin arrays[4] with the ultimate goal of creating devices that can efficiently capture light. To achieve this goal, an efficient interaction between the porphyrin molecules is required. This interaction can be achieved by connecting a large number of porphyrins by means of covalent bonds.[5]

Another, perhaps more attractive, approach is to use non-covalent interactions, for example, hydrogen bonding,[6] metal–ligand coordination,[7] solvophobic[8] and surface effects,[9] to construct ordered porphyrin arrays. Such an approach leads to the thermodynamically most stable structure and has the possibility of spontaneous self-repair. In the case of porphyrin self-assembly, metal–axial ligand interactions are an attractive construction tool because this type of interaction is highly directional and strong enough to generate stable structures, but still allows rearrangements and self-repair to take place. The affinity to bind one or more ligands strongly depends on the nature of the central metal in the porphyrin. Zinc–porphyrins (ZnPs) have been widely used to probe the binding characteristics of metalloporphyrins with ligands because they can be readily studied by both UV-visible and NMR spectroscopies. In general, ZnPs are pentacoordinate, and thus, bind nitrogen-containing ligands exclusively to one face of the porphyrin, which simplifies their coordination behaviour when compared with other metalloporphyrins, such as manganese, tin or iron porphyrins, which can bind axial ligands to both faces. Interesting ligands are those that are bidentate or multivalent because they can coordinate in between two ZnPs and impose a specific geometry onto the resulting complex, thereby also influencing communication between the porphyrins. Bidentate

[a] Dr. M. C. Lensen, Dr. J. A. A. W. Elemans, S. J. T. van Dingenen, J. W. Gerritsen, Prof. S. Speller, Prof. A. E. Rowan, Prof. R. J. M. Nolte
Institute for Molecules and Materials
Radboud University Nijmegen
Toernooiveld 1
6525 ED Nijmegen (The Netherlands)
Fax: (+31) 24-365-2929
E-mail: J.Elemans@science.ru.nl
A.Rowan@science.ru.nl

[b] Dr. M. C. Lensen
Current address:
DWI an der RWTH Aachen e.V.
Pauwelsstraße 8, 52074 Aachen (Germany)

ligands, such as 1,4-diaza[2,2,2]bicyclooctane (DABCO) or 4,4′-bipyridine (BIPY), have been used to construct "ladder complexes" from linear[10] or cyclic[11] porphyrin oligomers. Some of these structures display interesting non-linear optical properties.[10c]

In this paper we describe the synthesis and physical properties of giant disk-like porphyrin arrays, namely, porphyrin dodecamers $\mathbf{1}H_2$ and Zn–**1**,[12] which have two parallel faces of six porphyrins, each of which can be addressed individually by the coordination of axial ligands. The self-assembly of the dodecamers at liquid–solid interfaces has been studied at the submolecular level by means of scanning tunnelling microscopy (STM), and we have shown that by coordinating bidentate ligands to Zn–**1** the distance between the porphyrin molecules on the surface can be precisely controlled.

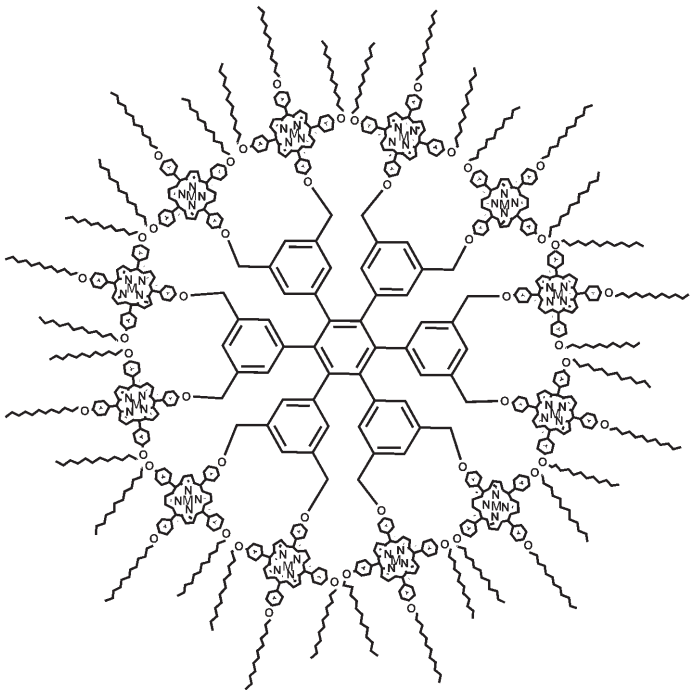

$\mathbf{1}H_2$ M = 2H
Zn–**1** M = Zn

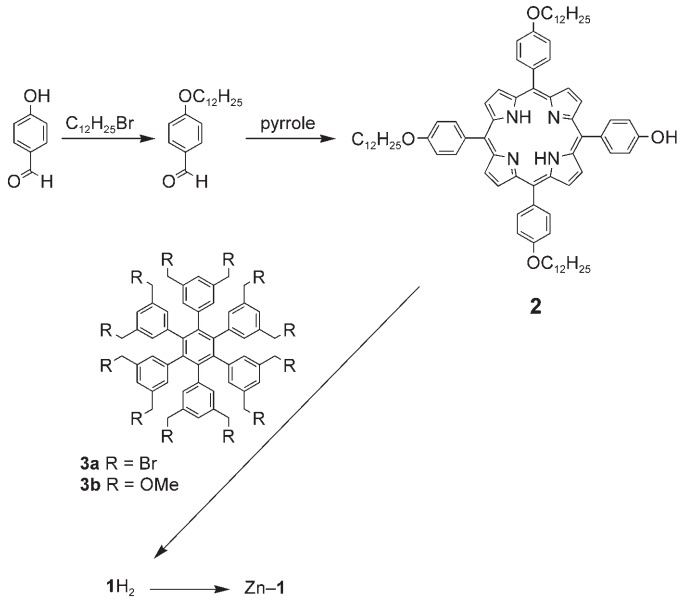

Scheme 1.

Results and Discussion

Synthesis and characterisation: Porphyrin dodecamer $\mathbf{1}H_2$ was synthesised from monohydroxy-substituted porphyrin **2** and extended aromatic core **3a**[13] in a yield of 55%, which is remarkably high for a 12-fold substitution reaction (Scheme 1). This high yield suggests that during the alkylation reaction a significant templating effect occurs in which the coupling of a porphyrin molecule to the core is favoured when other porphyrin moieties are already attached. Such a templating effect can be understood by taking into account the fact that the porphyrin moieties within the dodecamer are in close proximity and exert π–π stacking interactions during the coupling reactions.[14] In favour of this mechanism is the fact that only the dodecamer and no lower molecular weight oligomers are formed as reaction products. The macromolecule could be easily separated from its precursors by size-exclusion column chromatography. Zinc dodecamer Zn–**1** was obtained in 86% yield after metallation of $\mathbf{1}H_2$ with zinc acetate dihydrate. MALDI-TOF ($\mathbf{1}H_2$: *m*/*z* 14896 amu; Zn–**1**: *m*/*z* 15712 amu), gel permeation chromatography (GPC) and elemental analysis confirmed the identity and purity of both compounds.

When compared with the spectrum of precursor porphyrin **2**, the resonances in the ^{1}H NMR spectrum of $\mathbf{1}H_2$ (500 MHz, $CDCl_3$) are severely broadened (Figure 1c). The increased complexity of the spectrum further indicates a considerable level of dissymmetry in the molecule. With the help of extensive 1D and 2D NMR studies, in combination with molecular modelling calculations, the three-dimensional structure of $\mathbf{1}H_2$ could be determined (Figure 1a). The porphyrin dodecamer is proposed to adopt a unique yo-yo-like shape in which two disks that each contain six porphyrin moieties are stacked in an offset geometry to provide the molecule with an extended, flat π surface with a diameter of 38 and a thickness of 8 Å. The proposed geometry is based on several observations in the ^{1}H NMR spectrum of $\mathbf{1}H_2$. In the ^{1}H NMR spectrum of **2** (Figure 1c (top)), the proton signals of the three peripheral (two *cis* and one *trans*) porphyrin *meso*-phenyl substituents are found at the same chemical shifts (as AX quartets) and also the signals of the *cis*- and *trans*-OCH_2 groups resonate at the same chemical shift (as a sharp triplet), whereas in the spectrum of $\mathbf{1}H_2$ (Figure 1c (bottom)) they all become inequivalent and much broader. This inequivalency is further expressed by the signal for the β-pyrrole protons, which is a singlet in the spectrum of **2**, but has split into four broad signals in the spectrum of $\mathbf{1}H_2$. The signals for the protons of the *cis*-substituents showed large upfield shifts, which indicated their

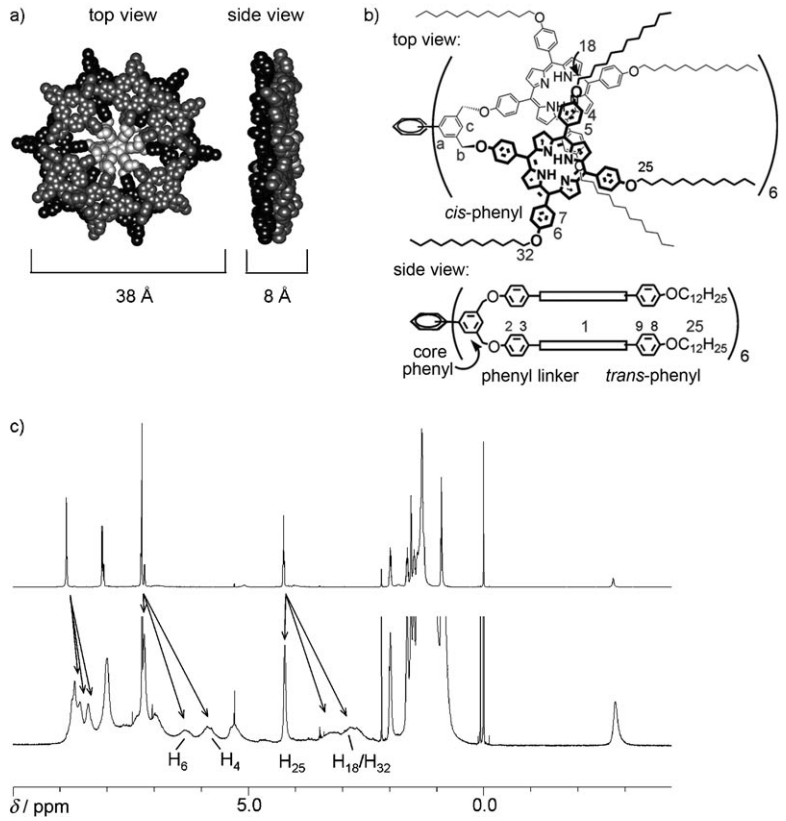

Figure 1. a) Top and side view of a molecular model of $\mathbf{1}H_2$ based on results from NMR studies. The alkyl tails have been omitted for clarity. b) Top and schematic side view of part of the molecule of $\mathbf{1}H_2$ highlighting the protons that are most relevant to the NMR studies. c) ^{1}H NMR spectra of **2** (top) and $\mathbf{1}H_2$ (bottom) in $CDCl_3$. The arrows indicate the most prominent shifts going from **2** to $\mathbf{1}H_2$. Proton numbering is shown in Figure 1b.

Table 1. ^{1}H NMR chemical shifts [ppm] of **3b**, **2** and $\mathbf{1}H_2$ and $\Delta\delta$ values [ppm] between signals in the spectra of $\mathbf{1}H_2$ and their reference compounds.[a]

Proton[b]	**3b**[c]	**2**	$\mathbf{1}H_2$	$\Delta\delta$
core H_a	6.70		7.59	+0.89
core H_c	6.61		8.04	+1.43
benzyl H_b	3.99		5.3	+1.31
phenyl linker H_2		6.86	7.2	+0.34
phenyl linker H_3		7.91	8.0	+0.09
cis-phenyl H_4		7.14	5.9	−1.24
cis-phenyl H_6			6.4	−0.74
cis-phenyl H_5		8.01	7.0	−1.01
cis-phenyl H_7		8.01	7.4	−0.61
trans-phenyl H_8		7.17	7.2	+0.03
trans-phenyl H_9		8.04	8.0	−0.04
cis-OCH_2 H_{18}		4.11	2.7	−1.43
cis-OCH_2 H_{32}		4.11	3.2	−0.91
trans-OCH_2 H_{25}		4.13	4.22	+0.09

[a] In $CDCl_3$, 500 MHz. [b] For proton numbering see Figure 1b. [c] See ref. [13].

strong shielding by a nearby porphyrin plane (Table 1). In contrast to these upfield shifts, the proton signals of the linking *meso*-phenyl ring shifted downfield. The same is true for the proton signals of the benzylic linkers and the aromatic core compared with these signals in dodecamethoxy derivative **3b**[13] (Table 1), which indicates that they are situated in the deshielding zone of the porphyrin. In the 2D NOESY spectrum of $\mathbf{1}H_2$, NOE contacts were observed between all of the porphyrin β-pyrrolic/pyrrole NH protons and the *cis*-phenyl-OCH_2 protons, however, NOE contacts between the porphyrin β-pyrrolic/pyrrole NH protons and the *trans*-phenyl-OCH_2 protons were not observed, which confirms that the *cis*-phenyl substituents are very close to the centre of an adjacent porphyrin (Figure 1b). Based on the observed shifts in the NMR spectrum and the NOE contacts, the geometry of $\mathbf{1}H_2$ was calculated by molecular modelling. (Figure 1a and b). The ^{1}H NMR and 2D NOESY spectra of Zn–**1** did not differ significantly from those of $\mathbf{1}H_2$. UV-visible spectroscopy in chloroform only revealed an overall broadening, but not a shift of the Soret absorption of $\mathbf{1}H_2$ and Zn–**1** when compared with their monomeric analogues, which suggests that there is a rather weak electronic communication between the porphyrin moieties. Upon diluting solutions of $\mathbf{1}H_2$ and Zn–**1** in $CDCl_3$ or [D_8]toluene from 10^{-3} to 10^{-5} M^{-1}, no significant changes were observed in their ^{1}H NMR spectra. In addition, both the Soret and Q absorption bands of the compounds in the UV-visible spectra in $CHCl_3$ or toluene followed Lambert–Beer behaviour upon varying their concentration from 5×10^{-6} to 8×10^{-8} M^{-1}. The combined ^{1}H NMR and UV-visible spectral behaviour indicates that over the concentration range of $\approx10^{-7}$–10^{-3} M^{-1} no significant aggregation of the porphyrin dodecamers occurs.[15]

Self-assembly at solid–liquid interfaces: The adsorption of $\mathbf{1}H_2$ and Zn–**1** from solution to the surface of highly oriented pyrolytic graphite (HOPG) was investigated by using scanning tunnelling microscopy (STM). Because of the presence of 36 C_{12}-alkyl group side chains on each dodecamer, it was expected that the lateral intermolecular interaction of these chains and their interactions with the hydrophobic HOPG substrate would drive the molecules to form well-ordered monolayer assemblies.[16] Indeed, immediately after the deposition of a drop of a concentrated solution of $\mathbf{1}H_2$ in 1-phenyloctane (1.0 mg in 50 μL, [$\mathbf{1}H_2$] = 1.3 mM) on a freshly cleaved HOPG (0001) surface, STM images showed the evolution of domains, with a size of several hundreds of

nanometers, of lamellar arrays of molecules (Figure 2a). During the initial scans the STM topographies were rather fuzzy, apparently owing to dynamic adsorption and re-dissolution of the molecules or a "liquid" state of the layer, but after approximately 30 min large domains of $\mathbf{1}H_2$ had formed that remained stable for hours during repeated scanning at a sufficiently low tunnelling current ($\approx$1 pA).[17] The domains of arrays of $\mathbf{1}H_2$ were oriented under angles of approximately 120°, which indicates that the molecules are commensurate with the hexagonal symmetry of the underlying graphite surface (Figure 2b). Apart from some defects, most of the lamellae in the 2D assembly were positioned at an equal distance of (43 ± 1) Å with a width of (34 ± 1) Å for the bright stripes within the lamellar pattern, which is in accordance with the diameter of the aromatic surface of the computer modelled structure of $\mathbf{1}H_2$ (see Figure 1a). The dark parts between the stripes are probably occupied by the alkyl chains and are unresolved.[18] Close examination of a magnification of the lamellae revealed that they contain a segmented fine structure (Figure 2c). The observed distances are in full agreement with an arrangement of the molecules of $\mathbf{1}H_2$ orthogonal to the surface in an edge-on orientation.[19] The ability of electron tunnelling to occur through a layer that is more than 5 nm in thickness highlights the remarkable conductivity of the molecules. The periodicity of the segments in the lamellae, as determined from the STM profiles, is (6.3 ± 0.3) Å. This distance is too small to incorporate one edge-on oriented molecule of $\mathbf{1}H_2$ because its calculated thickness is 8 Å. Therefore, we propose that each segment comprises one half of the double disk of a dodecamer, that is, two segments constitute one dodecamer molecule (namely, the black and grey halves of one molecule shown in Figure 1a).

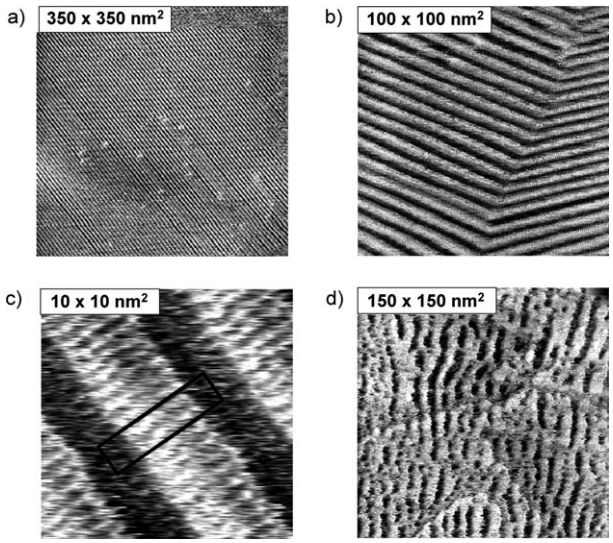

Figure 2. STM constant current images of $\mathbf{1}H_2$ (in all cases $I=1$ pA, $V_{bias}=-225$ mV). a) Large domain of columnar stacks at the 1-phenyloctane–HOPG interface. b) Two domains oriented at angle of 120°. c) Magnification of the stacks to show their segmented structure. The rectangle drawn on the image is proposed to contain one molecule of $\mathbf{1}H_2$. d) Fibre-like arrays of $\mathbf{1}H_2$ at the 1-phenyloctane–Au(111) interface. Note that the fibres are not interrupted by the clearly visible surface steps.

The self-assembly behaviour of $\mathbf{1}H_2$ was also investigated at the interface of 1-phenyloctane and Au(111). Fibre-like aggregates were observed, which were oriented in more or less parallel directions (Figure 2d). The apparent width of the fibres (ca. 7–9 nm) was not well-defined, and in several cases it was observed that several fibres combined to form thicker structures. It is also proposed that within these fibre-like aggregates the molecules of $\mathbf{1}H_2$ are oriented in an edge-on geometry to the surface. On Au(111), the affinity of the aggregates to the surface seems to be much weaker than on HOPG, which is indicated by a less well-defined alignment of the lamellae on Au(111), whereas the surface lattice is expressed in the direction of the aggregates on HOPG. Such behaviour is expected because alkyl chains are generally commensurate with HOPG, but not with Au(111) surfaces. Within the lamellae on Au(111) no molecular resolution could be observed, however, the interaction between the molecules of $\mathbf{1}H_2$ must still be quite strong because the fibre-like aggregates continue over surface steps without being interrupted.

To our surprise, Zn–**1** did not form stable adlayers at the interface of 1-phenyloctane and HOPG (1.0 mg in 50 μL, [Zn–**1**] = 1.3 mM).[20] Apparently, the intermolecular π–π stacking interactions between the porphyrin surfaces of Zn–**1** are not as strong as those between the aromatic surfaces of $\mathbf{1}H_2$. This difference is attributed to the fact that the zinc ion within a porphyrin molecule always requires an axial ligand. We tentatively propose that these axial ligands (e.g., water molecules present in the solvent) are coordinated to the zinc ions at the exterior of Zn–**1**, and thus inhibit, or at least diminish, favourable edge-on packing of the molecules in a stable 2D assembly.

Tuning the assemblies by axial-ligand binding: We investigated the possibility of inducing self-assembly of Zn–**1** by the addition of bidentate N-donor axial ligands. These ligands generally bind several orders of magnitude more strongly to ZnPs than water molecules, and hence, they are expected to expel the latter. In addition, their bidentate nature enables them to act as linkers between the molecules of Zn–**1**, which forces the assembly process in the direction of stable columnar arrays. Indeed, whereas the deposition of a droplet of pure Zn–**1** in 1-phenyloctane on an HOPG surface did not afford stable 2D assemblies, the addition of excess ($\approx$10 equiv) of DABCO to the solution resulted in the instantaneous formation of large domains of very stable lamellae of the complex, which were limited only by the HOPG domain size (Figure 3a). The coordination complexes[21] are arranged in similar columnar stacks as those observed for $\mathbf{1}H_2$, one difference is that the disk-like segments of the molecules of Zn–**1** in the complex are positioned at a slightly larger distance than those of $\mathbf{1}H_2$ (i.e., 8.2 ± 0.3 instead of 6.3 Å). In addition, the internal submolecular structure within the lamellae differed significantly from that observed for $\mathbf{1}H_2$. The bright stripes of the

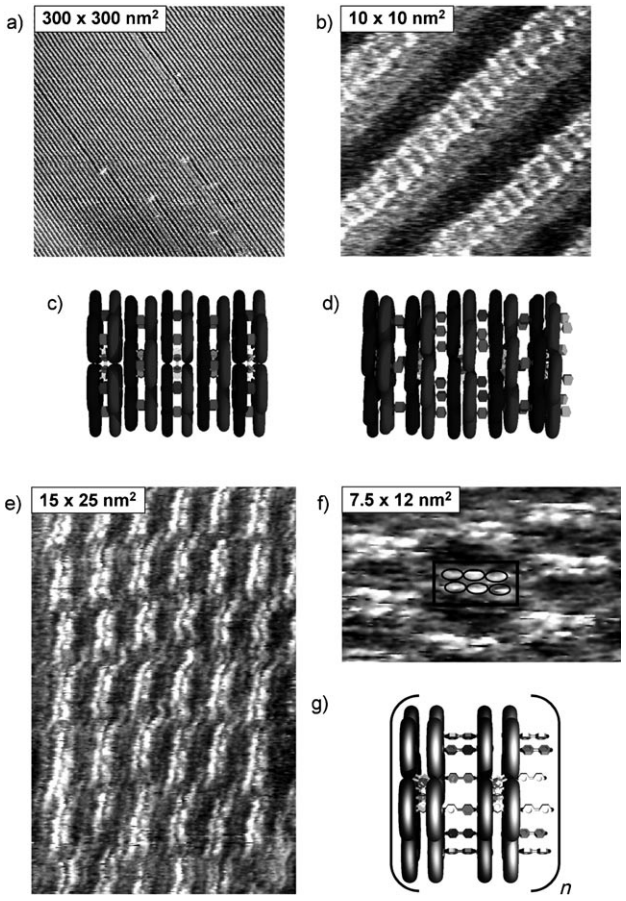

Figure 3. STM constant current images of the complex between Zn–**1** and DABCO (in both cases $I=1$ pA, $V_{bias}=-225$ mV) showing an overview of a large domain (a) and a magnification of the columnar stacks (b), which shows dumbbell-like moieties within the stack that are proposed to correspond to a single porphyrin within the dodecamer. c) The intramolecular binding mode of DABCO in which six DABCO ligands bind within the two disk-like moieties of Zn–**1** in a sandwich-like manner. d) The intermolecular binding mode of DABCO in which the DABCO ligands connect two molecules of Zn–**1**. It is proposed that within the porphyrin dodecamer stacks both modes of ligand binding occur, or that for the STM images an average between the two modes is imaged. STM constant current images of the complex between Zn–**1** and BIPY (in both cases $I=1$ pA, $V_{bias}=-180$ mV) that show e) a domain of the complex in which the yo-yo-like shape of Zn–**1** can be clearly recognised, and f) a magnification that shows the six oval spots in each molecule of Zn–**1** that are proposed to correspond to six porphyrins in the dodecamer. g) Schematic representation of the structure of the complex with six molecules of BIPY bridging two molecules of Zn–**1**.

DABCO-linked arrays, which consist of the aromatic parts of the molecules, are clearly built up from highly resolved, dumbbell-like moieties that are flanked by much more vague segments (Figure 3b). The dumbbell-like moieties have dimensions that correspond to the size of one porphyrin molecule that is imaged at its edge. It is proposed that this very high resolution is caused by the fact that the DABCO ligands bridge the ZnPs and freeze their conformations. As all dumbbell-like moieties are observed at an identical distance, it is believed that DABCO can bind both intramolecularly, that is, in a sandwich-like geometry, between the two disks of one molecule of Zn–**1** (Figure 3c) and intermolecularly between two adjacent molecules (Figure 3d). The intramolecular, sandwich-like binding mode could be demonstrated by using UV-visible spectroscopy. Upon the addition of DABCO to a solution of Zn–**1** (2×10^{-7} M) in chloroform, the Soret band sharpened and shifted from 424 to 427 nm, which is indicative of a coordination process (Figure 4a). The presence of clear isosbestic points in both the Soret and Q-band regions indicated that during the addition of the ligand only one distinct DABCO:Zn–**1** complex is formed. The titration curve levelled off after the addition of about six equivalents of the ligand (Figure 4c), which is a strong indication for the formation of a well-defined 6:1 complex between DABCO and Zn–**1** in which the six DABCO ligands are incorporated between the two porphyrin disks that constitute one dodecamer molecule. Assuming that non-cooperative binding of the six DABCO ligands between the two disks comprising one Zn–**1** molecule occurs (although this is probably a simplification), the UV-visible titration curve could be fitted to an association constant of $K_a=2\times10^7\,M^{-1}$ per ZnP–DABCO–ZnP unit, which highlights a strong sandwich-like binding mode. For entropic reasons, intermolecular coordination in which DABCO ligands bridge two or more Zn–**1** molecules is not expected at submicromolar concentrations. In a tightly packed monolayer at a liquid–solid interface, however, the concentration is much higher and intermolecular coordination of DABCO is also expected to occur. It can also be expected that at this interface association and dissociation of DABCO within the arrays is fast on the STM scanning timescale, therefore, it is possible that as a result an average between the two binding modes is observed. On the other hand, the simultaneous occurrence of both intra- and intermolecular binding modes within the porphyrin dodecamer stacks is equally possible.

As the addition of DABCO to Zn–**1** resulted in an increase in the distance between the porphyrin disks, the possibility that such metal–ligand coordination could be generally applied to control the surface self-assembly of the molecules was investigated. Instead of DABCO (N–N distance 2.6 Å), 4,4′-bipyridine (BIPY, N–N-distance 7.2 Å) was added to a solution of Zn–**1** in 1-phenyloctane. Molecular modelling studies indicated that this larger ligand cannot be bound to Zn–**1** in the sandwich-like geometry that was observed for the binding of DABCO. To investigate the binding behaviour of BIPY, UV-visible spectra were recorded of a solution of Zn–**1** (2×10^{-7} M) in chloroform to which the ligand was added. Upon its addition, the Soret band shifted from 424 to 428 nm and sharpened somewhat (Figure 4b), but the spectral changes were far less pronounced than those observed in the titration of Zn–**1** with DABCO. In addition, no well-defined isosbestic points were observed in the Soret band region. The titration curve levelled off after the addition of $\approx$12 equivalents of BIPY (Figure 4d) in contrast to only 6 for DABCO, which clearly indicates that no sandwich complexes are being formed and that the ligands bind independently to the 12 ZnPs of the dodecamer. From

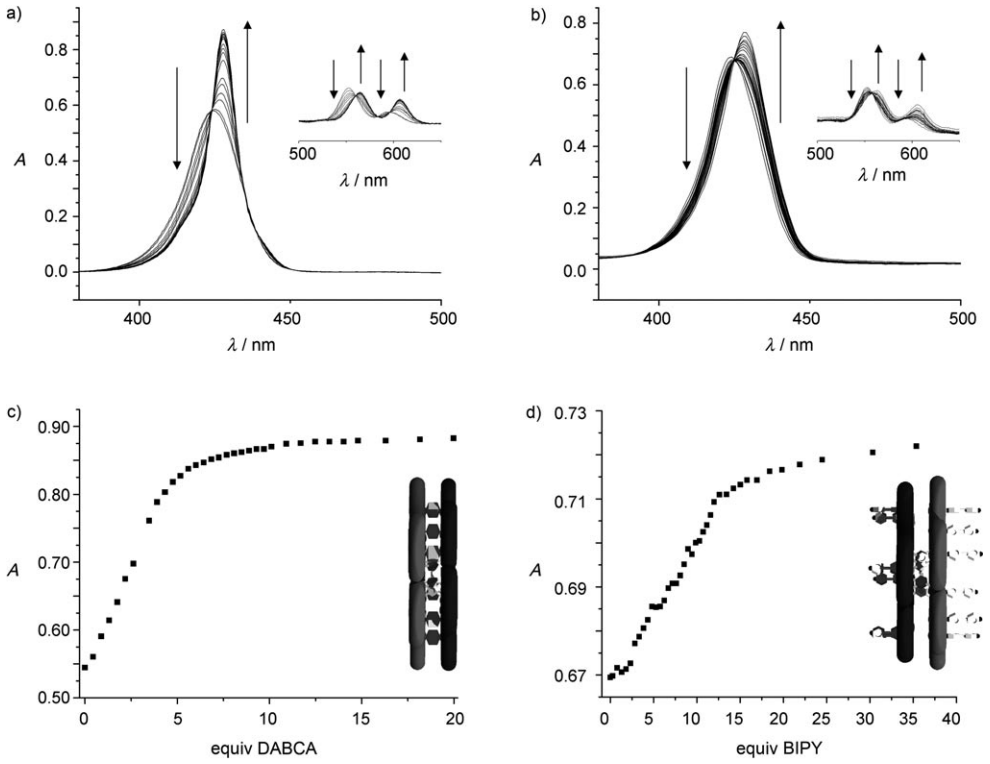

Figure 4. UV/Vis titrations of Zn–**1** with bidentate ligands (in $CHCl_3$, 296 K). a) Changes in the UV/Vis spectrum upon the addition of DABCO to Zn–**1**. b) Changes in the UV/Vis spectrum upon the addition of BIPY to Zn–**1**. c) Titration curve following the absorption at 428 nm and a schematic image of the proposed 1:6 sandwich-like complex between Zn–**1** and DABCO. d) Titration curve following the absorption at 426 nm and a schematic image of the proposed 1:12 complex in which the BIPY ligands bind independently to the porphyrin moieties of Zn–**1**.

the UV-visible titration curve no reliable association constant could be determined.

Imaging the metal–ligand complex at the liquid–solid interface of 1-phenyloctane and HOPG appeared to be highly dependent on the stoichiometry of the components. More specifically, only the application of a Zn–**1**/BIPY ratio of 1:6 resulted in the observation of domains, albeit relatively small ($<100\times100\ nm^2$), of stable monolayers of the coordination complex.[21] Individual edge-on molecules of Zn–**1** could be discerned, and their proposed yo-yo-like shape could now be clearly distinguished (Figure 3e). The centres of the molecules of Zn–**1** were at an average mutual distance of (28 ± 2) Å, with the two disk-like segments of one dodecamer stacked together closely. Close examination of the segments revealed that within each of them three oval spots were present that are proposed to correspond to the three porphyrin moieties in the top half of a disk imaged from above (Figure 3f). These observations corroborate the expectation that the BIPY ligands exclusively bind intermolecularly and act as linkers between the dodecamer molecules to rigidify their conformation at the surface, which is shown by their increased submolecular resolution (Figure 3g). As in the case of the complex of Zn–**1** with DABCO, the ligands themselves could not be imaged by STM probably owing to their dynamic association and dissociation with the surface.

Conclusion

We have demonstrated that large cyclic porphyrin arrays can be synthesised in a relatively high yield. We have been able to visualise these giant, disk-like molecules in extended edge-on oriented arrays at the interfaces of 1-phenyloctane with HOPG or Au(111). The distance between the porphyrin disks could be controlled by the addition of bidentate coordinating axial ligands that control the supramolecular architecture formed by metal–ligand interactions. Such a precise and unique control over surface organisation, as well as its characterisation by visualisation with STM, is essential for future applications of these porphyrin assemblies. Current research is focused on manipulating the porphyrin dodecamers further either by adding other coordinating ligands, for example, chiral ligands that can induce chirality into the arrays, or by replacing the Zn^{II} ions by Mn^{III}, Cu^{II} or Pt^{II} ions, which can provide the molecules and self-assembled arrays with magnetic, photophysical and catalytic properties.

Experimental Section

DMF was stored over BaO for 7 d and distilled under reduced pressure. CH_2Cl_2 and $CHCl_3$ were distilled from CaH_2. All commercial chemicals were used as received. TLC analysis was performed by using Merck

$60F_{254}$ silica plates. Merck silica gel 60H and Acros silica gel 60 were used for column chromatography and BioRad BioBeads SX-1 were used for size-exclusion chromatography. NMR spectra were recorded by using Bruker DPX200, AC300, FDRX500 and Varian Inova400 instruments. UV/Vis spectra were measured by using a Varian Cary 50 Conc spectrophotometer at ambient temperature and MALDI-TOF spectra were measured by using a Bruker Biflex III spectrometer in the linear mode. Samples for MALDI-TOF analysis were prepared by mixing 10 μL of dilute solutions ($\approx 10^{-5}$ M) of the porphyrin derivatives in chloroform with equal amounts of a matrix solution (dithranol; 20 mg mL^{-1}) in chloroform and depositing 3 μL droplets of the mixture on the sample plate. GPC measurements were performed by using a Shimadzu HPLC system equipped with a PL gel 5 μm guard column and a PL gel 5 μm mixed D column (Polymer Laboratories) with differential refractive index (38 °C) and UV (423 nm) detection by using THF as an eluent with a flow of 1 mL min^{-1} at $T = 35$ °C. Elemental analyses were measured by using a Carbo Erba EA 1108 instrument. Molecular modelling calculations were performed on a Silicon Graphics Indigo II work station by using the CHARMm force field.[22]

UV/Vis titrations: The first stock solution of Zn–**1** was prepared by dissolving a known amount of this molecule in distilled chloroform. This solution was used as the solvent for the second stock solution in which the ligand molecule was present. The amount of ligand originally weighed was calculated so that the second stock solution contained the ligand in a known excess with respect to Zn–**1**. Aliquots of the second stock solution were added to a measured amount of the first stock solution. The UV/Vis spectra were recorded immediately after mixing and the measured absorbance was plotted versus the calculated value for the number of equivalents of ligand added.

Scanning tunnelling microscopy: STM measurements were carried out in the constant current mode by using a homemade low-current scanning tunnelling microscope. HOPG surfaces were freshly cleaved, and Au(111) surfaces were prepared by the epitaxial growth of a gold film (thickness 100–200 nm) on freshly cleaved mica, at a pressure of $\approx 5 \times 10^{-7}$ mbar, after which the films were annealed at 200–300 °C for at least 2 h at $\approx 5 \times 10^{-8}$ mbar. STM tips were mechanically cut from a Pt/Ir (80:20) wire. A drop of an almost saturated solution of the compounds or their complexes in 1-phenyloctane (in all cases 1 mg of **1**H_2 or Zn–**1** in 50 μL of 1-phenyloctane) was brought onto the surface. Typically, an STM image (1024 lines × 1024 points) was recorded over a period of 10 min. All STM experiments were carried out at least in duplicate and the raw data were processed only by the application of a background flattening. Before and after the experiments the piezo element was calibrated in situ by lowering the bias voltage to 100 mV and raising the tunnelling current to 50 pA, which allowed imaging of the HOPG surface underneath the molecules.

***p*-Dodecoxybenzaldehyde**: *p*-Hydroxybenzaldehyde (14.2 g, 116 mmol) and 1-bromododecane (46.7 g, 188 mmol) were dissolved in DMF (75 mL). K_2CO_3 (50 g, 0.36 mol) was added and the reaction mixture was heated at reflux for 16 h. After cooling and filtration, the solution was concentrated and the product was purified by recrystallisation from ice cold methanol to give the product as a white solid (20 g, 59 %). ^{1}H NMR (200 MHz, $CDCl_3$): $\delta = 9.88$ (s, 1H; CHO), 7.83 (d, ^3J(H,H) = 8.8 Hz, 2H; *o*-ArH), 6.99 (d, ^3J(H,H) = 8.8 Hz, 2H; *m*-ArH), 4.04 (t, ^3J(H,H) = 6.5 Hz, 2H; OCH_2 H8), 1.82 (quintet, ^3J(H,H) = 7.8 Hz, 2H; OCH_2CH_2), 1.27 (br m, 14H; CH_2), 1.03 (d, ^3J(H,H) = 5.4 Hz, 2H; $CH_2CH_2CH_3$), 1.01 (d, ^3J(H,H) = 5.4 Hz, 2H; CH_2CH_3), 0.88 ppm (t, ^3J(H,H) = 6.5 Hz, 3H; CH_3); MS (EI): *m*/*z*: 290 [M^+]; elemental analysis calcd (%) for $C_{19}H_{30}O_2$: C 78.57, H 10.41; found: C 78.35, H 10.65.

5-(*p*-Hydroxyphenyl)-10,15,20-tris-(*p*-dodecoxyphenyl))porphyrin (2): Pyrrole (5.45 g, 81 mmol) was added to a mixture of *p*-hydroxybenzaldehyde (2.46 g, 20.2 mmol) and *p*-dodecoxybenzaldehyde (17.4 g, 60.0 mmol) in propionic acid (250 mL) and heated at reflux. After heating at reflux for 1.5 h under an N_2 atmosphere, the solvent was evaporated and the residue was purified by column chromatography (eluent: CH_2Cl_2). The second fraction was collected to give **2** as a purple solid (1.6 g, 7 %). ^{1}H NMR (400 MHz, $CDCl_3$): $\delta = 8.83$ (m, β-pyrrole, H10–17; 8H), 8.04 (d, ^3J(H,H) = 8.7 Hz, 6H; *o*-ArH H5, 7, 9), 7.98 (d, ^3J(H,H) = 8.7 Hz, 6H; *o*-ArH H3), 7.20 (d, ^3J(H,H) = 8.7 Hz, 6H; *m*-ArH H4, 6, 8), 7.03 (d, ^3J(H,H) = 8.4 Hz, 2H; *m*-ArH *H2*), 4.18 (t, ^3J(H,H) = 6.5 Hz, 6H; OCH_2), 1.95 (quintet, ^3J(H,H) = 6.2 Hz, 6H; OCH_2CH_2), 1.60 (quintet, ^3J(H,H) = 7.5 Hz, 6H; $OCH_2CH_2CH_2$), 1.30 (m, 48H; CH_2), 0.89 (t, ^3J(H,H) = 6.6 Hz, 9H; CH_3), −2.75 ppm (s, 2H; NH); ^{13}C NMR (75 MHz, $CDCl_3$): $\delta = 158.9$ (COR *cis*, *trans*), 155.2 (COH), 135.6 (C3), 134.7 (C9), 134.4 (C5, 7), 131 (C10–17), 119.9 (C2), 113.5 (C8), 112.7 (C4, 6), 68.3 (OCH_2), 32.0 (OCH_2CH_2), 29.8 (CH_2), 29.71 (CH_2), 29.69 (CH_2), 29.6 (CH_2), 29.5 (CH_2), 29.4 (CH_2), 26.3 (CH_2), 22.7 (CH_2), 14.2 ppm (CH_3); MS (FAB): *m*/*z*: 1183 [M+H]$^+$; elemental analysis calcd (%) for $C_{80}H_{102}N_4O_4$: C 81.17, H 8.69, N 4.73; found: C, 81.36, H 8.47, N 4.75.

Porphyrin dodecamer 1H$_2$: Hexakis([3,5-bis(bromomethyl)phenyl]benzene **3a**[13] (10.7 mg, 6.53 μmol) was added to a solution of **2** (180 mg, 152 μmol) in distilled DMF (10 mL). For 1.5 h nitrogen was passed through the solution. The solution was heated to 90 °C and K_2CO_3 (133 mg, 961 μmol) was added. The reaction mixture was heated to 130 °C and stirred for 3 d, after which the reaction was stopped and the DMF was removed in vacuo. The product was purified by column chromatography and subsequently by size-exclusion column chromatography (eluent: CH_2Cl_2) to give **1**H_2 as a purple solid (53 mg, 3.59 μmol, 55 %). M.p. 127 °C; ^{1}H NMR (500 MHz, $CDCl_3$, for proton numbering see graphic): $\delta = 8.75$ (brs, 24H; H17, H10), 8.7 (brs, 24H; H14, H13), 8.6 (brs, 24H; H15–16), 8.4 (brs, 24H; H12, H11), 8.03 (brs, 6H; Hc), 8.0 (brd, 48H; H9, H3), 7.59 (brs, 12H; Ha), 7.4 (brs, 24H; H7), 7.2 (brd, 48H, H8; H2), 7.0 (brs, 24H; H5), 6.4 (brs, 24H; H6), 5.9 (brs, 24H; H4), 5.3 (brs, 24H; Hb), 4.22 (brt, 24H; H25), 3.2 (brs, 24H; H32), 2.7 (brt, 24H; H18), 1.99 (brquartet, 24H; H26), 1.63 (brs, 24H; H27), 1.5–0.0 (brs, 192H; H28–30), 1.5–0.0 (brs, 240H; H33-H37), 1.5–0.0 (brs, 240H; H19–23), 0.9–0.8 (brt, 36H; H24), 0.87 (brt, 36H; H31), 0.87 (brt, 36H; H38), −2.78 ppm (brs, 24H; H1); ^{13}C NMR (75 MHz, $CDCl_3$): $\delta =$ 136 (C9, C3), 135 (C7), 134 (C5), 129.0 (Cc), 128.2 (Ca), 113 (C2), 112.6 (C8), 111 (C6), 110 (C4), 70.6 (Cb), 68.3 (C25), 67.9 (C32), 67.4 (C18), 32.0 (C36, C29, C22), 29.8 (C26), 29.7 (C35, C28, C21), 26.8 (C27), 26.5 (C33, C20, C19), 26 (C34), 23.0 (C37, C30, C23), 14.1 ppm (C38, C31, C24); UV/Vis ($CHCl_3$): λ_{max} (log ε): 423 (6.6), 520 (5.3), 558 (5.2), 595 (4.8), 653 nm (4.9 M^{-1} cm^{-1}); MS (MALDI-TOF): *m*/*z*: 14896; elemental analysis calcd (%) for $C_{1014}H_{1254}N_{48}O_{48}$: C 81.83, H 8.49, N 4.52; found: C 81.73, H 8.46, N 4.65.

ZnP dodecamer Zn–1: To a solution of **1**H_2 (0.012 g, 0.81 μmol) in chloroform (10 mL) and methanol (5 mL) zinc(II) acetate dihydrate (0.017 g, 75.6 μmol) was added. The solution was refluxed for 16 h. After cooling, the solution was washed with water (3x). The solvent was evaporated and the product was purified on a silica column (size 0.035 mm–

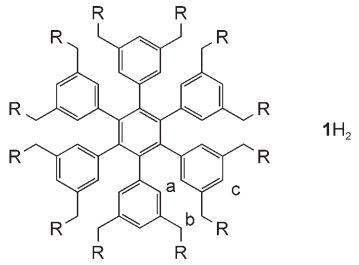

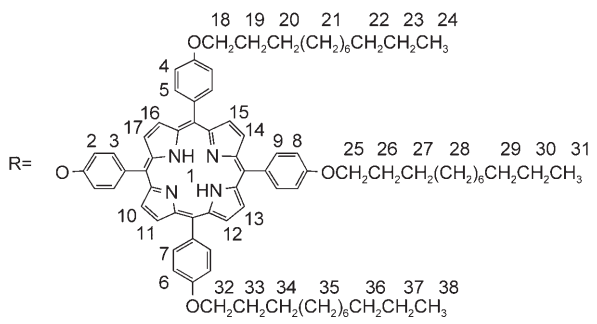

0.070 mm, pore size 6 nm, eluent: 1% methanol and 1% triethylamine in chloroform). Yield: 11 mg (0.70 μmol, 86%) of Zn–**1** as a purple solid. M.p. 129°C; ^{1}H NMR (500 MHz, $CDCl_3$): $\delta = 8.7$ (brs, 48H; H17, H10, H14, H13), 8.6 (brs, 24H; H15–16), 8.4 (brs, 24H; H11–12), 7.99 (brs, 6H; Hc), 7.97 (brd, 48H; H9, H3), 7.62 (brs, 12H; Ha), 7.51 (brs, 24H; H7), 7.23 (brd, 24H; H2), 7.22 (brd, 24H; H8), 7.16 (brs, 24H; H5), 6.5 (brs, 24H; H6), 6.1 (brs, 24H; H4); 5.3 (brs, 24H; Hb), 4.24 (brt, 24H; H25), 3.4 (brt, 24H; H32), 3.0 (brt, 24H; H18), 1.98 (brquartet, 24H; H26), 1.67 (brs, 24H; H27), 1.5–0.0 (brs, 192H; H30, H29, H28), 1.5–0.0 (brs, 240H; H33-H37), 1.5–0.0 (brs, 240H; H23-H19), 0.87 ppm (brt, 108H; H38, H31, H24); ^{13}C NMR (75 MHz, $CDCl_3$): $\delta = 135$ (C9, C3, C7, C5), 132 (Cc), 120 (Ca), 113 (C2), 112.5 (C8), 112 (C6, C4), 68.3 (Cb), 68.0–67.4 (C25, C32, C18), 31.9 (C36, C29, C22), 29.6 (C26), 29.4 (C35, C28, C21), 26.3 (C27), 26.0 (C33, C20, C19, C34), 22.7 (C37, C30, C23), 14.1 ppm (C38, C31, C24); UV/Vis ($CHCl_3$): λ_{max} (log ε): 424 (6.7), 522 (5.6), 580 nm ($5.1\,M^{-1}cm^{-1}$); MS (MALDI-TOF): m/z: 15644 (calcd 15712); elemental analysis (%) calcd for $C_{1014}H_{1230}N_{48}O_{48}Zn_{12}$: C 77.85, H 7.92, N 4.30; found: C 77.68, H 8.22, N 4.16.

Acknowledgements

The Dutch National Research School Combination Catalysis (NRSC-C), support by NanoNed—the Dutch nanotechnology initiative by the Ministry of Economic Affairs and the Council for the Chemical Sciences of the Netherlands Organization for Scientific Research (CW-NWO) are acknowledged for financial support to M.C.L., S.S., R.J.M.N., J.A.A.W.E. (VENI grant) and A.E.R. (VIDI grant). We would like to thank Dr. H. Engelkamp for his help with drawing the cartoons.

[1] For a recent review, see: J. A. A. W. Elemans, R. van Hameren, R. J. M. Nolte, A. E. Rowan, *Adv. Mater.* **2006**, *18*, 1251.

[2] a) E. G. McRae, M. Kasha, *J. Chem. Phys.* **1958**, *28*, 721; b) M. Kasha, H. R. Rawls, M. A. El-Bayoumi, *Pure Appl. Chem.* **1965**, *11*, 371.

[3] a) G. McDermott, S. M. Prince, A. A. Freer, A. M. Hawthornthwaite-Lawless, M. Z. Papiz, R. J. Cogdell, N. W. Isaacs, *Nature* **1995**, *374*, 517; b) T. Pullerits, V. Sundström, *Acc. Chem. Res.* **1996**, *29*, 381; c) S. Bahatyrova, R. N. Frese, C. A. Siebert, J. D. Olsen, K. O. van der Werf, R. van Grondelle, R. A. Niederman, P. A. Bullough, C. Otto, C. N. Hunter, *Nature* **2004**, *430*, 1058.

[4] For reviews about artificial porphyrin arrays, see: a) M. R. Wasielewski, *Chem. Rev.* **1992**, *92*, 435; b) H. Kurreck, M. Huber, *Angew. Chem.* **1995**, *107*, 929; *Angew. Chem. Int. Ed. Engl.* **1995**, *34*, 849; c) C. Chin-Ti in *Comprehensive Supramolecular Chemistry, Vol. 5* (Eds.: J. L. Atwood, J. E. D. Davies, D. D. MacNicol, F. Vögtle, D. N. Reinhoudt, J.-M. Lehn), Pergamon, Elmsford, **1996**, p. 91; d) J. K. M. Sanders in *Comprehensive Supramolecular Chemistry, Vol. 9* (Eds.: J. L. Atwood, J. E. D. Davies, D. D. MacNicol, F. Vögtle, D. N. Reinhoudt, J.-M. Lehn), Pergamon, Elmsford, **1996**, p. 131; e) A. Harriman, J. P. Sauvage, *Chem. Soc. Rev.* **1996**, *25*, 41; f) M. D. Ward, *Chem. Soc. Rev.* **1997**, *26*, 365; g) C. M. Drain, G. Bazzan, T. Milic, M. Vinodu, J. C. Goeltz, *Isr. J. Chem.* **2005**, *45*, 724; h) A. Satake, Y. Kobuke, *Tetrahedron* **2005**, *61*, 13.

[5] a) A. K. Burrell, D. L. Officer, P. G. Plieger, D. C. W. Reid, *Chem. Rev.* **2001**, *101*, 2751; b) D. Kim, A. Osuka, *Acc. Chem. Res.* **2004**, *37*, 735.

[6] a) C. M. Drain, K. C. Russell, J.-M. Lehn, *Chem. Commun.* **1996**, 337; b) C. M. Drain, X. X. Shi, T. Milic, F. Nifiatis, *Chem. Commun.* **2001**, 287; c) Y. H. Ni, R. R. Puthenkovilakom, Q. Huo, *Langmuir* **2004**, *20*, 2765.

[7] a) U. Michelsen, C. A. Hunter, *Angew. Chem.* **2000**, *112*, 780; *Angew. Chem. Int. Ed.* **2000**, *39*, 764; b) K. Ogawa, Y. Kobuke, *Angew. Chem.* **2000**, *112*, 4236; *Angew. Chem. Int. Ed.* **2000**, *39*, 4070; c) C. A. Hunter, C. M. R. Low, M. J. Packer, S. E. Spey, J. G. Vinter, M. O. Vysotsky, C. Zonta, *Angew. Chem.* **2001**, *113*, 2750; *Angew. Chem. Int. Ed.* **2001**, *40*, 2678; d) R. Takahashi, Y. Kobuke, *J. Am. Chem. Soc.* **2003**, *125*, 2372; e) Y. Kuramochi, A. Satake, Y. Kobuke, *J. Am. Chem. Soc.* **2004**, *126*, 8668; f) O. Shoji, H. Tanaka, T. Kaway, Y. Kobuke, *J. Am. Chem. Soc.* **2005**, *127*, 8598; g) D. Furutsu, A. Satake, Y. Kobuke, *Inorg. Chem.* **2005**, *44*, 4460.

[8] a) J. M. Ribo, J. Crusats, F. Sague, J. Claret, R. Rubires, *Science* **2001**, *292*, 2063; b) A. D. Schwab, D. E. Smith, C. S. Rich, E. R. Young, W. F. Smith, J. C. de Paula, *J. Phys. Chem. B* **2003**, *107*, 11339; c) M. de Napoli, S. Nardis, R. Paolesse, M. G. H. Vicente, R. Lauceri, R. Purrello, *J. Am. Chem. Soc.* **2004**, *126*, 5934; d) M. Yuasa, K. Oyaizu, A. Yamaguchi, M. Kuwakado, *J. Am. Chem. Soc.* **2004**, *126*, 11128; e) G. de Luca, A. Romeo, L. Monsù Scolaro, *J. Phys. Chem. B* **2005**, *109*, 7149; f) Z. Wang, C. J. Medforth, J. A. Shelnutt, *J. Am. Chem. Soc.* **2004**, *126*, 15954; g) J.-S. Hu, Y.-G. Guo, H. P. Liang, L.-J. Wan, L. Jiang, *J. Am. Chem. Soc.* **2005**, *127*, 17090.

[9] a) T. Yokoyama, S. Yokoyama, T. Kamikado, Y. Okuno, S. Mashiko, *Nature* **2001**, *413*, 619; b) T. N. Milic, N. Chi, D. G. Yablon, G. W. Flynn, J. D. Batteas, C. M. Drain, *Angew. Chem.* **2002**, *114*, 2221; *Angew. Chem. Int. Ed.* **2002**, *41*, 2117; c) A. D. Schwab, D. E. Smith, B. Bond-Watts, D. E. Johnston, J. Hone, A. T. Johnson, J. C. de Paula, W. F. Smith, *Nano Lett.* **2004**, *4*, 1261; d) Y. Zhou, B. Wang, M. Zhu, J. G. Hou, *Chem. Phys. Lett.* **2005**, *403*, 140; e) J. Otsuki, E. Nagamine, T. Kondo, K. Iwasaki, M. Asakawa, K. Miyake, *J. Am. Chem. Soc.* **2005**, *127*, 10400; f) R. van Hameren, P. Schön, A. M. van Buul, J. Hoogboom, S. V. Lazarenko, J. W. Gerritsen, H. Engelkamp, P. C. M. Christianen, H. A. Heus, J. C. Maan, T. Rasing, S. Speller, A. E. Rowan, J. A. A. W. Elemans, R. J. M. Nolte, *Science* **2006**, *314*, 1433.

[10] a) H. L. Anderson, *Inorg. Chem.* **1994**, *33*, 972; b) P. N. Taylor, H. L. Anderson, *J. Am. Chem. Soc.* **1999**, *121*, 11538; c) T. E. O. Screen, J. R. G. Thorne, R. G. Denning, D. G. Bucknall, H. L. Anderson, *J. Am. Chem. Soc.* **2002**, *124*, 9712.

[11] a) V. F. Slagt, P. W. N. M. van Leeuwen, J. N. H. Reek, *Angew. Chem.* **2003**, *115*, 5777; *Angew. Chem. Int. Ed.* **2003**, *42*, 5619; b) P. Ballester, A. I. Oliva, A. Costa, P. M. Deyà, A. Frontera, R. M. Gomila, C. A. Hunter, *J. Am. Chem. Soc.* **2006**, *128*, 5560.

[12] Part of this work has appeared as a preliminary communication: M. C. Lensen, S. J. T. van Dingenen, J. A. A. W. Elemans, H. P. Dijkstra, G. P. M. van Klink, G. van Koten, J. W. Gerritsen, S. Speller, R. J. M. Nolte, A. E. Rowan, *Chem. Commun.* **2004**, 762.

[13] H. P. Dijkstra, C. A. Kruithof, N. Ronde, R. van de Coevering, D. J. Ramon, D. Vogt, G. P. M. van Klink, G. van Koten, *J. Org. Chem.* **2003**, *68*, 675.

[14] H. A. M. Biemans, A. E. Rowan, A. Verhoeven, P. Vanoppen, L. Latterini, J. Foekema, A. Schenning, E. W. Meijer, F. C. de Schryver, R. J. M. Nolte, *J. Am. Chem. Soc.* **1998**, *120*, 11054.

[15] For a detailed study of the assembly of porphyrin dodecamers in ring-like aggregates and their absorption and fluorescence behaviour, see: C. R. L. P. N. Jeukens, M. C. Lensen, F. J. P. Wijnen, J. A. A. W. Elemans, P. C. M. Christianen, A. E. Rowan, J. W. Gerritsen, R. J. M. Nolte, J. C. Maan, *Nano Lett.* **2004**, *4*, 1401.

[16] X. Qiu, C. Wang, Q. Zeng, B. Xu, S. Yin, H. Wang, S. Xu, C. Bai, *J. Am. Chem. Soc.* **2000**, *122*, 5550.

[17] An increase in tunnelling current to values above 1 pA resulted in an instantaneous loss of ordered structures in the STM images.

[18] In general, bright features in STM images correspond to parts of the molecule that are good conductors of the tunnelling current, for example, an aromatic surface. For further information, see: R. Lazzaroni, A. Calderone, J. L. Bredás, J. P. Rabe, *J. Chem. Phys.* **1997**, *107*, 99.

[19] For other examples of "edge-on" oriented disk-like molecules that have been imaged by STM, see: a) P. Samorì, H. Engelkamp, P. de Witte, A. E. Rowan, R. J. M. Nolte, J. P. Rabe, *Angew. Chem.* **2001**, *113*, 2410; *Angew. Chem. Int. Ed.* **2001**, *40*, 2348; b) C. B. France, P. G. Schroeder, B. A. Parkinson, *Nano Lett.* **2002**, *2*, 693; c) J. A. A. W. Elemans, M. C. Lensen, J. W. Gerritsen, H. van Kempen, S. Speller, R. J. M. Nolte, A. E. Rowan, *Adv. Mater.* **2003**, *15*, 2070.

[20] Experimental data and molecular modelling calculations have shown that π-π stacking interactions between ZnPs are stronger than between free base porphyrins. For more information, see: C. A. Hunter, J. K. M. Sanders, *J. Am. Chem. Soc.* **1990**, *112*, 5525.
[21] The coordination of the axial ligands to Zn–**1** was clearly evidenced by a colour change of the solution from purple to green upon their addition.
[22] CHARMm version 22.0, Revision 92.0911, Resident and Fellows of Harvard College, **1984**, **1992**, with the use of template charges.

Received: January 17, 2007
Published online: July 4, 2007

